

# Generalized Shortcuts to Adiabaticity and Enhanced Robustness Against Decoherence

Alan C. Santos<sup>\*</sup> and Marcelo S. Sarandy<sup>†</sup>

*Instituto de Física, Universidade Federal Fluminense,  
Av. Gal. Milton Tavares de Souza s/n, Gragoatá, 24210-346 Niterói, Rio de Janeiro, Brazil*

Shortcuts to adiabaticity provide a general approach to mimic adiabatic quantum processes via arbitrarily fast evolutions in Hilbert space. For these counter-diabatic evolutions, higher speed comes at higher energy cost. Here, we provide a minimal energy demanding counter-diabatic theory. As a by-product, we show that this general approach can be used to obtain infinite classes of transitionless models, including time-independent Hamiltonians under certain conditions over the eigenstates of the original Hamiltonian. We apply these results to investigate shortcuts to adiabaticity in decohering environments by introducing the requirement of a fixed energy resource. In this scenario, we show that generalized transitionless evolutions can be more robust against decoherence than their adiabatic counterparts. We illustrate this enhanced robustness both for the Landau-Zener model and for quantum gate Hamiltonians.

PACS numbers: 03.67.-a, 03.67.Ac, 03.67.Hk

The adiabatic theorem [1–3] constitutes a successful strategy for eigenstate tracking in quantum information and quantum control (see, e.g., Ref. [4]). It states that a system initially prepared in an eigenstate of a time-dependent Hamiltonian  $H(t)$  will evolve to the corresponding instantaneous eigenstate at a later time  $T$ , provided that  $H(t)$  varies smoothly and that  $T$  is much larger than a power of the relevant minimal inverse energy gap (see, e.g., Ref. [5–9]). In a real open-system scenario, the performance of the adiabatic dynamics is upper bounded by the competition between the adiabatic time scale, which is favored by a slow evolution, and the typically short decoherence time scales. This interplay provides an optimal time scale for adiabatic processes in decohering environments [10, 11].

The adiabatic dynamics can be reproduced by generalized transitionless evolutions obtained via shortcuts to adiabaticity [12–14]. Such accelerated processes allow us to derive an exact adiabatic evolution at an arbitrary finite time. Shortcuts to adiabaticity have been used to speed up adiabatic processes in a number of applications, e.g. tracking of many-body systems across quantum phase transitions [15, 16], quantum gate Hamiltonians [17–19], heat engines in quantum thermodynamics [20], among others (e.g., Refs. [21–23]). The robustness of such transitionless evolutions has recently been studied through different experimental architectures, as nitrogen-vacancy setups [24], trapped ions [25], atoms in cavities [26], nuclear magnetic resonance (NMR) [27], and optomechanics [28]. Naturally, the speed of the evolution is constrained by the energy cost of the implementation, with faster evolutions being more energy demanding [17]. By providing identical energy resources at a finite evolution time  $\tau$ , a fundamental problem is then whether shortcuts to adiabaticity can provide a more efficient performance in terms of fidelity than their adiabatic counterparts by adjusting its pace within the decoherence time scales. Here, we address this question

by considering a general counter-diabatic theory, which can be optimized for a minimum energy consumption. As a by-product, we apply this general approach to obtain infinite classes of transitionless models, including time-independent Hamiltonians under certain conditions over the eigenstates of the original (adiabatic) Hamiltonian. Concerning robustness against decoherence, we consider Markovian open systems and impose fixed energy resources. This is a key point, since unlimited energy provides arbitrarily fast dynamics already for adiabatic evolution, through an arbitrarily large gap between the ground and first excited states. It is then shown that a supremacy of the counter-diabatic dynamics can always be achieved by adjusting the evolution rate. This is illustrated in the Landau-Zener model and in quantum gate Hamiltonians.

*Generalized counter-diabatic theory and energy cost* — The starting point for the counter-diabatic theory is the evolution operator  $U(t)$ , which can be defined as (see, e.g., Ref. [29])

$$U(t) = \sum_n e^{i \int_0^t \theta_n(\xi) d\xi} |n_t\rangle \langle n_0|, \quad (1)$$

where  $\theta_n(t)$  is a set of arbitrary real phases [30, 31] and  $\{|n_t\rangle = |n(t)\rangle\}$  is the set of eigenstates of the original (adiabatic) Hamiltonian  $H_0(t)$ . Let us assume that the quantum system is initially prepared in a specific eigenstate  $|k_0\rangle$  of  $H_0(t)$ , namely,  $|\psi(0)\rangle = |k_0\rangle$ . Then, the Hamiltonian  $H_{SA}(t) = -iU(t)\dot{U}^\dagger(t)$ , which denotes the *shortcut to the adiabatic* Hamiltonian  $H_0(t)$ , evolves the system to its instantaneous eigenlevel  $|\psi(t)\rangle = e^{i \int_0^t \theta_k(\xi) d\xi} |k_t\rangle$ . Explicitly, we write  $H_{SA}(t)$  as ( $\hbar = 1$ )

$$H_{SA}(t) = i \sum_n (|\dot{n}_t\rangle \langle n_t| + i\theta_n(t) |n_t\rangle \langle n_t|). \quad (2)$$

The functions  $\theta_n(t)$  have originally been identified with the adiabatic phase  $\theta_n(t) = -E_n(t) + i\langle n_t | \dot{n}_t \rangle$  [32], which exactly mimics an adiabatic evolution. In this

particular case, we can write  $H_{\text{SA}}(t)$  as  $H_0(t) + H_{\text{CD}}(t)$ , where  $H_0(t) = \sum_n E_n(t) |n_t\rangle\langle n_t|$  is the Hamiltonian that drives the adiabatic dynamics and  $H_{\text{CD}}(t) = i \sum_n (|\dot{n}_t\rangle\langle n_t| + \langle \dot{n}_t|n_t\rangle |n_t\rangle\langle n_t|)$  is the *counter-diabatic* Hamiltonian. However, there is a number of situations for which we need not exactly mimic an adiabatic process, but only assure that the system is kept in an instantaneous energy eigenstate (independently of its quantum phase) [17–26, 28, 33, 34]. The dynamics in terms of arbitrary phases  $\theta_n(t)$  will be denoted as a generalized *transitionless* evolution. These phases can be nontrivially optimized in transitionless evolutions in terms of its energy cost. We adopt as a measure of energy cost the average Hilbert-Schmidt norm of the Hamiltonian throughout the evolution, which is given by [17, 35, 36]

$$\Sigma_{\text{SA}}(\tau) = \frac{1}{\tau} \int_0^\tau \sqrt{\text{Tr}[H_{\text{SA}}^2(t)]} dt, \quad (3)$$

where  $\tau$  denotes the total evolution time. In particular,  $\tau$  can be set by the quantum speed limit [37], which allows for arbitrarily fast dynamics, which are bounded only by the energy cost required for such an evolution [17, 36]. The energy cost in a transitionless evolution can be minimized by a suitable choice of the  $\theta_n(t)$ . Remarkably, this optimization can be analytically derived, which is established by Theorem 1 below. Its derivation is provided in Appendix A.

**Theorem 1.** *Consider a closed quantum system under adiabatic evolution governed by a Hamiltonian  $H_0(t)$ . The energy cost to implement its generalized transitionless counterpart, driven by the Hamiltonian  $H_{\text{SA}}(t)$ , can be minimized by setting  $\theta_n(t) = \theta_n^{\text{min}}(t) = -i\langle \dot{n}_t|n_t\rangle$ .*

In particular, for any evolution such that the quantum parallel-transport condition is verified [32], the energy cost to implement a transitionless evolutions is always optimized by choosing  $\theta_n^{\text{min}}(t) = 0$ . As a by-product, the generalized counter-diabatic theory can be used as a tool to yield time-independent Hamiltonians for transitionless evolutions. In general, the Hamiltonian  $H(t)$  has its form constrained both by the choice of the phases  $\theta_n(t)$  and by eigenstates of the adiabatic Hamiltonian  $H_0(t)$ . Thus, we can delineate under what conditions we can choose the set  $\{\theta_n(t)\}$  in order to obtain a time-independent Hamiltonian for a transitionless evolution. To answer this question, we impose  $\dot{H}_{\text{SA}}(t) = 0$  considering arbitrary phases  $\theta_n(t)$ . This leads to Theorem 2 below. Its derivation is provided in Appendix B.

**Theorem 2.** *Let  $H_0(t)$  be a discrete quantum Hamiltonian, with  $\{|m_t\rangle\}$  denoting its set of instantaneous eigenstates. If  $\{|m_t\rangle\}$  satisfies  $\langle k_t|\dot{m}_t\rangle = c_{km}$ , with  $c_{km}$  complex constants  $\forall k, m$ , then a family of time-independent Hamiltonians  $H^{\{\theta\}}$  for generalized transitionless evolutions can be defined by setting  $\theta_m(t) = \theta$ , with  $\theta$  a single arbitrary real constant  $\forall m$ .*

*Transitionless dynamics under decoherence* — Theorems 1 and 2 ensure both an energetically optimal counter-diabatic evolution and families of possible time-independent transitionless Hamiltonians. A rather important point for the generalized counter-diabatic theory is whether it is robust against decoherence. The robustness of the counter-diabatic dynamics and inverse engineering schemes has recently been considered in the literature [38–41]. Here, in order to provide a comparison between adiabatic and generalized counter-diabatic dynamics, we will require identical energy resources for each implementation. More specifically, we will consider the performance of transitionless evolutions in open systems described by convolutionless master equations given by

$$d_s \rho(s) = -i\tau [H_{\text{SA}}(s), \rho(s)] + \tau \mathcal{L}_i[\rho(s)], \quad (4)$$

where  $\mathcal{L}_i[\rho(s)]$  describes the decohering contribution to the quantum dynamics, which is parametrized by the normalized time  $s = t/\tau$ , with  $\tau$  the total time of evolution and  $0 \leq s \leq 1$ . For Markovian evolution [42, 43], we have  $\mathcal{L}_i[\rho(s)] = \frac{1}{2} \sum_i \gamma_i^2(s) [2L_i(s)\rho(s)L_i^\dagger(s) - \{L_i^\dagger(s)L_i(s), \rho(s)\}]$ , with  $L_i(s)$  denoting Lindblad operators and  $\gamma_i(s)$  (positive) decoherence rates. Here, we will consider as an illustration Lindblad operators for generalized amplitude damping (GAD) in the eigenbasis of the Hamiltonian, which read

$$L_\pm^{\text{GAD}}(s) = U^\dagger(s) \sigma_\pm U(s), \quad (5)$$

where  $U(s)$  is the unitary operator that diagonalizes the Hamiltonian and  $\sigma_\pm = (\sigma_x \mp i\sigma_y)/2$ , with  $\{\sigma_x, \sigma_y, \sigma_z\}$  denoting Pauli matrices. The GAD channel describes dissipation to an environment at finite temperature. Its decoherence rates  $\gamma_+$  and  $\gamma_-$  are given by [44, 45]  $\gamma_+ = \sqrt{\gamma_0 N_{th}}$  and  $\gamma_- = \sqrt{\gamma_0 (N_{th} + 1)}$ , where  $\gamma_0$  is the spontaneous emission rate and  $N_{th}$  is the Planck distribution that gives the number of thermal photons at a fixed frequency. For simplicity, we adjust the temperature such that  $N_{th} = 1/2$  and define  $\gamma_0 \equiv \alpha\omega_r$ , with  $\alpha$  a dimensionless parameter and  $\omega_r$  an arbitrary (typically relevant) frequency associated with the quantum system. Then, we obtain  $\gamma_+ = \sqrt{\alpha\omega_r}/2$  and  $\gamma_- = \sqrt{3}\gamma_+$ . For equal energy resource provided for adiabatic and generalized transitionless evolutions,  $\omega_r$  will be taken as follows. We consider a set  $\{\tau_i | 1 \leq i \leq n\}$  of total evolution times. The total time  $\tau_i$  fixes the energy of the generalized transitionless evolution, with faster evolutions related to shorter times. For a given  $\tau_i$ , we adjust the corresponding frequency  $\omega_i$  of the Hamiltonian that drives the adiabatic evolution so that  $\Sigma_0(\tau_i) = \Sigma_{\text{SA}}(\tau_i)$ , with  $\Sigma_0(\tau_i)$  denoting the energy cost of the adiabatic model. The relevant frequency  $\omega_r$  that sets the decoherence rates  $\gamma_\pm$  will then be defined by the average of  $\omega_i$  for the values of  $\tau_i$  considered. More specifically,  $\omega_r \equiv \frac{1}{n} \sum_{i=1}^n \omega_i$ , with  $n = 200$  in our numerical treatment.

*Landau-Zener model* — As a first application, let us consider the dynamics of a two-level quantum system,

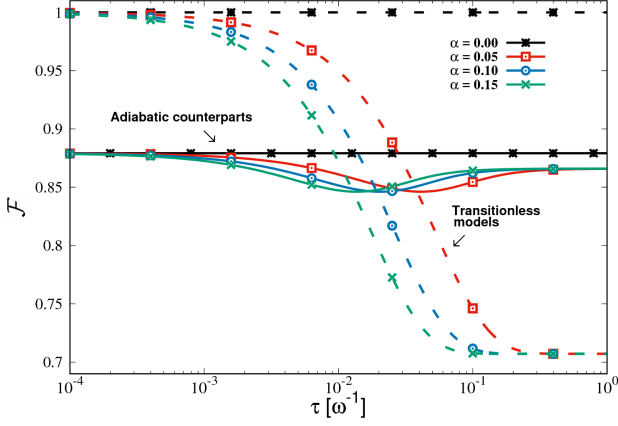


FIG. 1. Fidelity  $\mathcal{F}$  under GAD in the eigenstate basis for both adiabatic (continuum curves) and optimal transitionless dynamics (dashed curves) for identical energy cost in the Landau-Zener model. We set  $\vartheta_0 = \pi/3$ .

i.e., a qubit, evolving under the Landau-Zener Hamiltonian

$$H_0^{\text{LZ}}(s) = -\omega [\sigma_z + \tan \vartheta(s) \sigma_x], \quad (6)$$

with  $\tan \vartheta(s)$  a dimensionless time-dependent parameter. The system is initialized in the ground state  $|E_-(0)\rangle = |0\rangle$  of  $H_0^{\text{LZ}}(0)$ . By considering a unitary dynamics and a sufficiently large total evolution time (adiabatic time), the qubit evolves to the instantaneous ground state  $|E_-(s)\rangle = \cos(\vartheta(s)/2)|0\rangle + \sin(\vartheta(s)/2)|1\rangle$  of  $H_0^{\text{LZ}}(s)$ . It is possible to show that  $H_0^{\text{LZ}}(s)$  satisfies the requirement in Theorem 2 if, and only if we choose the linear interpolation  $\vartheta(s) = \vartheta_0 s$  (see Appendix C). Thus, we adopt this choice for simplicity. Moreover, we will be interested in the performance of the transitionless evolution with optimal energy resource so that we impose  $\theta_n(s)$  as in the Theorem 1. Thus, by considering adiabatic evolution through the Hamiltonian  $H_0^{\text{LZ}}(s)$ , the optimal energy resource is performed by setting  $\theta_n(s) = 0$  (see Appendix C). Consequently, we have  $H_{\text{SA}}(s) = (\vartheta_0/2\tau)\sigma_y$ .

We are now ready to compare the behavior under decoherence of both adiabatic and counter-diabatic models. To settle the problem in a fair scenario, we submit both models to the same requirements of energy cost and total evolution time  $\tau$ . We adopt the fidelity  $\mathcal{F}(\tau) = \langle E_-(1) | \rho(1) | E_-(1) \rangle$  as a success measure of each protocol, with  $\rho(1)$  denoting the solution of Eq. (4) at  $s = 1$ . The robustness of adiabatic and optimal transitionless evolutions under GAD are then shown in Fig. 1. The decoherence rate strength is controlled by the dimensionless parameter  $\alpha$ . The fidelity for unitary dynamics ( $\alpha = 0$ ) in the adiabatic model is constant and smaller than 1 because the requirement of fixed energy imposes a fixed relationship between  $\tau$  and  $\omega$ . This

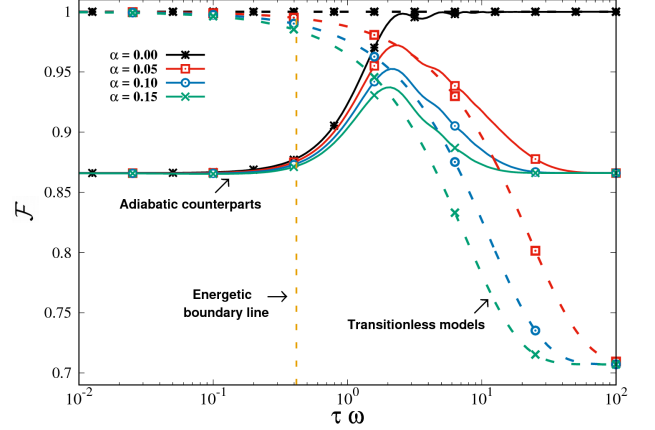


FIG. 2. Fidelity under GAD in the eigenstate basis for the adiabatic dynamics (continuum curves) and its optimal transitionless counterpart (dashed curves) under different energy resources in the Landau-Zener model. The vertical dashed line represents the boundary line between  $\Sigma_0(\tau) \leq \Sigma_{\text{SA}}(\tau)$  and  $\Sigma_0(\tau) \geq \Sigma_{\text{SA}}(\tau)$ , with  $\Sigma_0(\tau)$  and  $\Sigma_{\text{SA}}(\tau)$  denoting the adiabatic and optimal generalized transitionless energy cost, respectively. We set  $\vartheta_0 = \pi/3$ .

keeps the adiabatic condition unchanged as we increase  $\tau$ , since we will have to decrease  $\omega$  at the same pace. On the other hand, transitionless evolutions have fidelity close to 1, since they are *not* ruled by the adiabatic constraint. Remarkably, for non-unitary evolutions ( $\alpha > 0$ ), there exists a range of values for the total evolution time  $\tau$  for which generalized transitionless evolutions are more robust than their adiabatic counterparts. This result is also shown in Fig. 2, where we allow for different resource contents (for this case, the relevant frequency is simply adopted as  $\omega_r \equiv \omega$ ). Observe that the behavior of the fidelity curve on the right and left hand side of the vertical line shows that, even for more energy provided for the adiabatic model, the transitionless dynamics can be more robust than the adiabatic dynamics for a fixed  $\alpha$ . In general, the crossing points that establish the supremacy of the optimal counter-diabatic evolution are non-trivially derived. They depend on both the coupling strength  $\alpha$  and the decoherence channel (as discussed in Appendix C).

*Robustness of counter-diabatic QC* — Counter-diabatic evolutions can be used to speed up adiabatic quantum gates. More specifically, it has been applied to perform universal QC via either counter-diabatic controlled evolutions [17] or counter-diabatic quantum teleportation [18]. We will now show that counter-diabatic QC can be more robust against decoherence than its adiabatic counterpart. Our physical apparatus is now a bipartite system  $\mathcal{TA}$  composed by a target system  $\mathcal{T}$  with two qubits and a single qubit auxiliary system  $\mathcal{A}$ . In this scenario, let us consider an arbitrary rotation over a qubit of an angle  $\phi$  around a direction  $\hat{n}$  in the Bloch

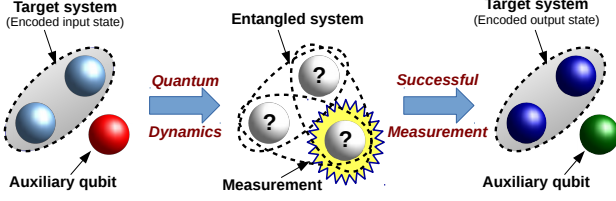


FIG. 3. Protocol for a probabilistic implementation of a controlled evolution in a two-qubit state. Before the quantum evolution (either adiabatic or nonadiabatic) the input state is encoded in the target system, while the ancilla qubit is initialized in  $|0\rangle$ . After the evolution, a measurement (in the computational basis) is performed on the auxiliary qubit. A successful measurement corresponds to the state  $|1\rangle$ . If the auxiliary qubit is found in the state  $|0\rangle$  after the measurement, the system returns to its initial state and the repetition of the process is required.

sphere controlled by another auxiliary qubit. The Hamiltonian that implements such a controlled rotation is given by  $H_{\text{SQC}}(s) = [\mathbb{1} - P_{11,\hat{n}_-}] \otimes H_0(s) + P_{11,\hat{n}_-} \otimes H_\phi(s)$ , where  $P_{11,\hat{n}_\pm} = |11\rangle\langle 11| \otimes |\hat{n}_\pm\rangle\langle \hat{n}_\pm|$  is a projector over  $\mathcal{T}$ , with  $|\hat{n}_\pm\rangle$  being a state in the direction  $\hat{n}$ , and the Hamiltonian  $H_\xi(s)$  ( $\xi = \{0, \phi\}$ ) acts on  $\mathcal{A}$ , reading [46]

$$H_\xi(s) = -\omega\{\sigma_z \cos(\varphi_0 s) + \sin(\varphi_0 s)[\sigma_x \cos \xi + \sigma_y \sin \xi]\},$$

with  $\varphi_0$  denoting an arbitrary parameter that sets the success probability of obtaining the desired state at the end of the evolution. This parameter plays a role in the energy performance of counter-diabatic QC, with probabilistic counter-diabatic QC ( $\varphi_0 \neq \pi$ ) being energetically more favorable than its deterministic ( $\varphi_0 = \pi$ ) counterpart [19]. A scheme of the protocol is provided in Fig. 3. To implement counter-diabatic quantum gates [17], we use the Hamiltonian  $H_{\text{SQC}}(s) = [\mathbb{1} - P_{11,\hat{n}_-}] \otimes H_0^{\text{SA}}(s) + P_{11,\hat{n}_-} \otimes H_\phi^{\text{SA}}(s)$ , where  $H_\xi^{\text{SA}}(s)$  is the Hamiltonian for generalized transitionless evolution associated with  $H_\xi(s)$ . Remarkably, each Hamiltonian  $H_\xi(s)$  satisfies the conditions required by Theorems 1 and 2, so that we can obtain an optimal time-independent Hamiltonian for a transitionless dynamics by choosing an evolution given by  $H_\xi^{\text{SA}} = \varphi_0/2\tau(\sigma_y \cos \xi - \sigma_x \sin \xi)$  (a derivation is provided in Appendix D).

To investigate the robustness of counter-diabatic QC, we choose the entangling CNOT gate as an illustration of our results. CNOT can be viewed as a controlled rotation of  $\pi$  around  $x$ -axis in the Bloch sphere, so that we set  $\phi = \pi$  and  $|\hat{n}_\pm\rangle = |\pm\rangle$ , with  $|\pm\rangle = (1/\sqrt{2})(|0\rangle + |1\rangle)$ . We consider the initial state  $|\psi(0)\rangle = |+\rangle|0\rangle$  and apply the gate Hamiltonian for CNOT to create a Bell state  $|\psi_{00}\rangle = (1/\sqrt{2})(|00\rangle + |11\rangle)$ . The system is non-unitarily evolved under GAD, with the same energy resource provided to the adiabatic and optimal transitionless model. The fidelity  $\mathcal{F}(\tau) = \sqrt{\langle \psi_{00} | \rho(1) | \psi_{00} \rangle}$  for the process is exhibited in Fig. 4. Remarkably, provided a fixed  $\alpha$ , the performance of probabilistic counter-diabatic QC, with

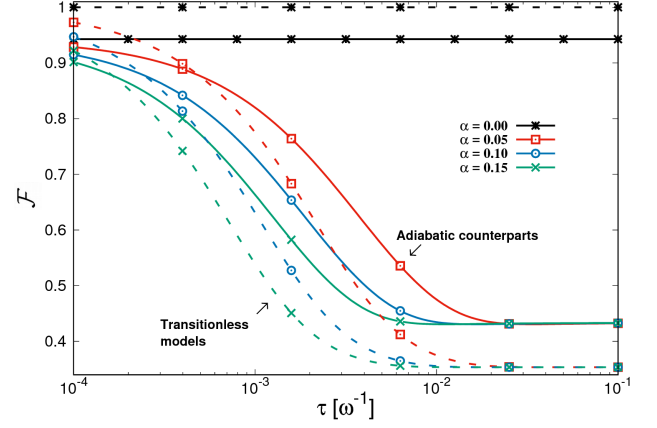


FIG. 4. Fidelity for implementation of the CNOT gate to the state  $|+\rangle|0\rangle$  via deterministic ( $\varphi_0 = \pi$ ) adiabatic QC (continuum lines) and probabilistic ( $\varphi_0 \approx 0.742\pi$ ) fast QC by optimal transitionless dynamics (dashed lines) for unitary and non-unitary evolutions under GAD for identical energy resources.

optimal energy cost, is more robust than its adiabatic counterpart in its optimal energy version ( $\varphi = \pi$ ) for a range of the total evolution time. Energy optimization in the optimal transitionless model is achieved for  $\varphi_0 \approx 0.742\pi$  for any  $\tau$ . For other gates or decoherence processes, this counter-diabatic advantage also happens for a specific range of time (see Appendix D). In any case, for equal resources provided, we can always find dynamical regimes where counter-diabatic processes are more robust against decoherence.

**Conclusions** — In summary, we have developed a generalized minimal energy demanding counter-diabatic theory, which is able to yield efficient shortcuts to adiabaticity via fast transitionless evolutions. Moreover, we have investigated the robustness of adiabatic and counter-diabatic dynamics under decoherence by introducing the requirement of fixed energy resources, so that a comparison is settled down in a fair scenario. Then, we have shown both for the Landau-Zener model and for quantum gate Hamiltonians that there always exist dynamical regimes for which generalized transitionless evolutions are more robust and therefore a preferred approach in a decohering setup. These results are encouraging for the generalized transitionless approach in the open system realm as long as local Hamiltonians are possible to be designed. In the specific case of quantum gate Hamiltonians, this approach can be applied, e.g. to derive robust local building blocks for analog implementations of quantum circuits (see, e.g., Refs. [47, 48]). Experimental realizations and generalized shortcuts via reservoir engineering are further directions left for future research.

**Acknowledgments** — We acknowledge Gonzalo Muga and Tameem Albash for useful discussions. A.C.S. is supported by CNPq-Brazil. M.S.S. acknowledges support



from CNPq-Brazil (No. 304237/2012-4), FAPERJ (No 203036/2016), and the Brazilian National Institute for Science and Technology of Quantum Information (INCT-IQ).

### Appendix A: Proof of Theorem 1

**Theorem 1.** Consider a closed quantum system under adiabatic evolution governed by a Hamiltonian  $H_0(t)$ . The energy cost to implement its generalized transitionless counterpart, driven by the Hamiltonian  $H_{SA}(t)$ , can be minimized by setting  $\theta_n(t) = \theta_n^{\min}(t) = -i\langle \dot{n}_t | n_t \rangle$ .

*Proof.* We adopt as a measure of energy cost the Hamiltonian Hilbert-Schmidt norm, which reads

$$\Sigma_{SA}(\tau) = \frac{1}{\tau} \int_0^\tau \sqrt{\text{Tr}[H_{SA}^2(t)]} dt, \quad (7)$$

Then, we obtain

$$H_{SA}^2(t) = \hbar^2 \sum_n \left[ |\dot{n}_t\rangle\langle \dot{n}_t| + \theta_n^2(t) |n_t\rangle\langle n_t| + i\theta_n(t) (|n_t\rangle\langle \dot{n}_t| - |\dot{n}_t\rangle\langle n_t|) \right]. \quad (8)$$

By taking the trace of  $H_{SA}^2(t)$  in Eq. (8), we have

$$\begin{aligned} \text{Tr}[H_{SA}^2(t)] &= \sum_m \langle m_t | H_{SA}^2(t) | m_t \rangle \\ &= \hbar^2 \sum_n \left[ \langle \dot{n}_t | \dot{n}_t \rangle + \theta_n^2(t) + 2i\theta_n(t) \langle \dot{n}_t | n_t \rangle \right]. \end{aligned} \quad (9)$$

Then

$$\Sigma_{SA}(\tau) = \frac{1}{\tau} \int_0^\tau \sqrt{\sum_n \langle \dot{n}_t | \dot{n}_t \rangle + \Gamma_n(\theta_n)} dt, \quad (10)$$

where we have  $\Gamma_n(\theta_n) = \theta_n^2(t) + 2i\theta_n(t) \langle \dot{n}_t | n_t \rangle$ .

We can now find out the functions  $\theta_n(t)$  that minimize the energy cost in transitionless evolutions. For this end, we minimize the quantity  $\Sigma_{SA}(\tau)$  for the Hamiltonian  $H_{SA}(t)$  with respect to parameters  $\theta_n(t)$ , where we will adopt it being independents. By evaluating  $\partial_{\theta_n} \Sigma(\tau)$ , we obtain

$$\partial_{\theta_n} \Sigma_{SA}(\tau) = \frac{1}{2\tau} \int_0^\tau \frac{\partial_{\theta_n} \{\text{Tr}[H_{SA}^2(t)]\}}{\sqrt{\text{Tr}[H_{SA}^2(t)]}} dt.$$

We then impose  $\partial_{\theta_n} \{\text{Tr}[H_{SA}^2(t)]\} = 0$  for all time  $t \in [0, \tau]$ , which ensures  $\partial_{\theta_n} \Sigma_{SA}(\tau) = 0$ . Thus, by using the Eq. (9), we write

$$\partial_{\theta_n} \{\text{Tr}[H_{SA}^2(t)]\} = 2\theta_n(t) + 2i\langle \dot{n}_t | n_t \rangle = 0. \quad (11)$$

This implies

$$\theta_n(t) = \theta_n^{\min}(t) = -i\langle \dot{n}_t | n_t \rangle. \quad (12)$$

From the second derivative analysis, it follows that the choice for  $\theta_n(t)$  as in Eq. (12) necessarily minimizes the energy cost, namely,  $\partial_{\theta_n}^2 \Sigma_{SA}(\tau) |_{\theta_n = \theta_n^{\min}} > 0$ , which concludes the proof.  $\square$

### Appendix B: Proof of Theorem 2

**Theorem 2.** Let  $H_0(t)$  be a discrete quantum Hamiltonian, with  $\{|m_t\rangle\}$  denoting its set of instantaneous eigenstates. If  $\{|m_t\rangle\}$  satisfies  $\langle k_t | \dot{m}_t \rangle = c_{km}$ , with  $c_{km}$  complex constants  $\forall k, m$ , then a family of time-independent Hamiltonians  $H^{\{\theta\}}$  for generalized transitionless evolutions can be defined by setting  $\theta_m(t) = \theta$ , with  $\theta$  a single arbitrary real constant  $\forall m$ .

*Proof.* By taking the time derivative of the Hamiltonian  $H_{SA}(t)$ , we obtain

$$\dot{H}_{SA}(t) = i \sum_n \frac{d}{dt} \left[ |\dot{n}_t\rangle\langle n_t| + i\theta_n(t) |n_t\rangle\langle n_t| \right]. \quad (13)$$

Then, the matrix elements of  $\dot{H}_{SA}(t)$  in the eigenbasis  $\{|m_t\rangle\}$  of the Hamiltonian  $H_0(t)$  read

$$\begin{aligned} \langle k_t | \dot{H}_{SA}(t) | m_t \rangle &= i\langle k_t | \ddot{m}_t \rangle + i \sum_n \langle k_t | \dot{n}_t \rangle \langle \dot{n}_t | m_t \rangle \\ &\quad - \left[ \dot{\theta}_k(t) \delta_{km} + \theta_m(t) \langle k_t | \dot{m}_t \rangle + \theta_k(t) \langle \dot{k}_t | m_t \rangle \right]. \end{aligned}$$

Now, by using  $\langle k_t | \dot{n}_t \rangle = -\langle \dot{k}_t | n_t \rangle$ , we write  $\langle k_t | \dot{n}_t \rangle \langle \dot{n}_t | m_t \rangle = \langle \dot{k}_t | n_t \rangle \langle n_t | \dot{m}_t \rangle$  and thus

$$\begin{aligned} \langle k_t | \dot{H}_{SA}(t) | m_t \rangle &= i \frac{d}{dt} [\langle k_t | \dot{m}_t \rangle] \\ &\quad - \left\{ \dot{\theta}_k(t) \delta_{km} + [\theta_m(t) - \theta_k(t)] \langle k_t | \dot{m}_t \rangle \right\}. \end{aligned} \quad (14)$$

For  $k = m$  in Eq. (14), we impose the vanishing of the diagonal elements of  $\dot{H}_{SA}(t)$ , namely,  $\langle k_t | \dot{H}_{SA}(t) | k_t \rangle = 0$ . This yields

$$\dot{\theta}_m(t) = i \frac{d}{dt} [\langle m_t | \dot{m}_t \rangle], \quad (15)$$

On the other hand, for  $k \neq m$  in Eq. (14), we now impose the vanishing of the off-diagonal elements of  $\dot{H}_{SA}(t)$ , namely,  $\langle k_t | \dot{H}_{SA}(t) | m_t \rangle = 0$  ( $k \neq m$ ). This yields

$$i \frac{d}{dt} [\langle k_t | \dot{m}_t \rangle] = [\theta_m(t) - \theta_k(t)] \langle k_t | \dot{m}_t \rangle \quad (k \neq m). \quad (16)$$

By taking  $\langle m_t | \dot{m}_t \rangle \equiv c_{mm}$  in Eq. (15), with  $c_{mm}$  denoting by hypothesis complex constants, we get  $\theta_m(t) = \theta_m(0) \equiv \theta_m$ , namely,  $\theta_m(t)$  is a constant function  $\forall m$ . Moreover, by using  $\langle k_t | \dot{m}_t \rangle \equiv c_{km}$  in Eq. (16), with  $c_{km}$  denoting *nonvanishing* complex constants, we obtain  $\theta_k = \theta_m$ ,  $\forall k, m$ . If  $c_{km} = 0$ , then  $\theta_k$  and  $\theta_m$  are not necessarily equal, but Eq. (16) will also be satisfied by this choice. Therefore, it follows that  $\theta_m(t)$  can be simply taken as

$$\theta_m(t) = \theta_m = \theta \quad \forall m, \quad (17)$$

with  $\theta$  a single real constant. This concludes the proof.  $\square$

### Appendix C: Transitionless evolution in Landau-Zener model

In this section, we discuss the details of the transitionless dynamics for the Landau-Zener Hamiltonian, whose Hamiltonian is  $H_0^{\text{LZ}}(s) = -\omega[\sigma_z + \tan \vartheta(s)\sigma_x]$ , with  $\tan \vartheta(s)$  a dimensionless time-dependent parameter. The instantaneous ground  $|E_-(s)\rangle$  and first excited  $|E_+(s)\rangle$  states of  $H_0^{\text{LZ}}(s)$  are

$$|E_-(s)\rangle = \cos\left[\frac{\vartheta(s)}{2}\right]|0\rangle + \sin\left[\frac{\vartheta(s)}{2}\right]|1\rangle, \quad (18)$$

$$|E_+(s)\rangle = -\sin\left[\frac{\vartheta(s)}{2}\right]|0\rangle + \cos\left[\frac{\vartheta(s)}{2}\right]|1\rangle. \quad (19)$$

#### Energy cost for the Landau-Zener model

From the form of the eigenstates  $|E_\pm(s)\rangle$  we can obtain the Hamiltonian for the generalized transitionless evolution associated with  $H_0^{\text{LZ}}(s)$ . For optimal energy cost, Eq. (12) establishes  $\theta_n(t) = \langle d_s E_\pm(s) | E_\pm(s) \rangle = 0$  for the states in Eqs. (18) and (19). Therefore, the optimal Hamiltonian  $H_{\text{SA}}(s)$  is given by  $H_{\text{SA}}(s) = H_{\text{CD}}^{\text{LZ}}(s)$ , with

$$H_{\text{CD}}^{\text{LZ}}(s) = \sum_{k=\pm} |d_s E_k(s)\rangle \langle E_k(s)| = \frac{d_s \vartheta(s)}{2\tau} \sigma_y. \quad (20)$$

From Eq. (20), it follows that a time-independent counter-diabatic Hamiltonian can be derived by imposing  $\vartheta(s) = \vartheta_0 s$ , with  $\vartheta_0$  denoting a real constant. Considering the energy cost for a Hamiltonian  $H(t)$  in the interval  $t \in [0, \tau]$  as provided by  $\frac{1}{\tau} \int_0^\tau \sqrt{\text{Tr}[H^2(t)]} dt$ , we get

$$\Sigma_0(\tau) = \sqrt{2}|\omega| \int_0^1 |\sec[\vartheta(s)]| ds, \quad (21)$$

$$\Sigma_{\text{SA}}(\tau) = \int_0^1 \frac{|d_s \vartheta(s)|}{\sqrt{2}\tau} ds = \frac{|\vartheta(1)|}{\sqrt{2}\tau}. \quad (22)$$

where  $\Sigma_0(\tau)$  and  $\Sigma_{\text{SA}}(\tau)$  are the energy costs for the adiabatic and optimal shortcut Hamiltonians, respectively. Remarkably, from Eqs. (21) and (22), it follows that the energy cost for the counter-diabatic Landau-Zener model is independent of the path followed by the system on the Bloch sphere, while its adiabatic counterpart depends on it. In particular, for obtaining  $\Sigma_{\text{SA}}(\tau)$ , we have used  $\tan \vartheta(0) = 0$  and, therefore,  $\vartheta(0) = 0$ . Note that there is a range of values for  $\tau$  for which the energy cost of the generalized transitionless dynamics is less than its adiabatic version. Indeed, by evaluating the relation between  $\Sigma_0(\tau)$  and  $\Sigma_{\text{SA}}(\tau)$  we get

$$\mathcal{R}(\tau) = \frac{\Sigma_0(\tau)}{\Sigma_{\text{SA}}(\tau)} = |\omega|\tau \frac{2 \int_0^1 |\sec[\vartheta(s)]| ds}{|\vartheta(1)|}. \quad (23)$$

By imposing identical energy cost, i.e.  $\mathcal{R}(\tau) = 1$ , we obtain

$$|\omega|\tau = \frac{|\vartheta(1)|}{2 \int_0^1 |\sec[\vartheta(s)]| ds}. \quad (24)$$

Therefore, identical energy cost can be obtained by adjusting  $\omega$  according to the total evolution time  $\tau$ , as in Eq. (23).

#### Robustness against decoherence in the Landau-Zener model

The system is prepared in the ground state  $|E_-(0)\rangle = |0\rangle$  of the Landau-Zener Hamiltonian  $H_0^{\text{LZ}}(s)$  at  $s = 0$ . Then, we let the system evolve aiming at the target state  $|E_-(1)\rangle$ . The behavior of the system under nonunitary evolution under the GAD channel has been presented in the main text. Here, we generalize the results by considering dephasing in the instantaneous eigenbasis of the Hamiltonian, whose Lindblad operator reads  $L_d(s) = U^\dagger(s)\sigma_z U(s)$ , with decoherence rate given by  $\gamma_d \equiv \alpha\omega_r$ . As before,  $\alpha$  denotes a dimensionless parameter and  $\omega_r$  a relevant frequency adopted to parametrize  $\gamma_d$ . The success of the protocol is measured by the fidelity  $\mathcal{F} = \sqrt{\langle E_-(1) | \rho(1) | E_-(1) \rangle}$ , with  $\rho(1)$  obtained from the solution of the master equation.

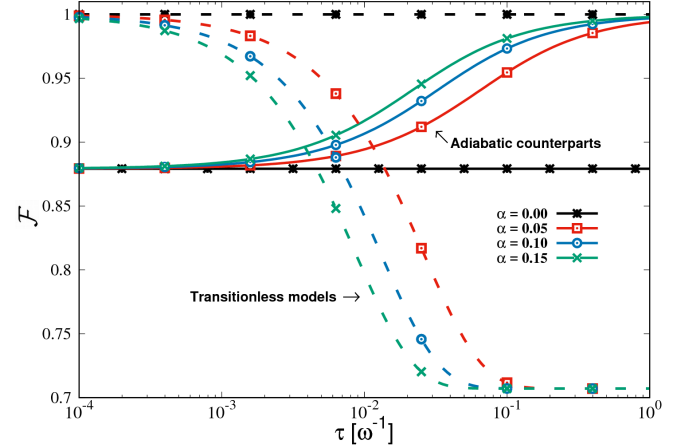


FIG. 5. Fidelity for the adiabatic Landau-Zener model (continuum lines) and its optimal transitionless counterpart (dashed lines) under dephasing, where the same energy resources for adiabatic and generalized transitionless evolutions are provided. We set  $\vartheta_0 = \pi/3$ .

The situation of identical energy resource for adiabatic and generalized transitionless evolutions is considered in Fig. 5, while the case of different energy resources are considered in Fig. 6. For both cases, there exists a range of values for the total evolution time  $\tau$  for which generalized transitionless evolutions are more robust than their

adiabatic counterparts. Notice that this occurs even by taking into account that dephasing in the eigenstate basis favors the adiabatic model over its generalized transitionless counterpart, since it only affects superpositions of eigenstates (not purely the ground state of the adiabatic Hamiltonian). Indeed, Figs. 5 and 6 show that fidelity improves in the asymptotic regime for the adiabatic case, with a negligible effect of dephasing for infinite time.

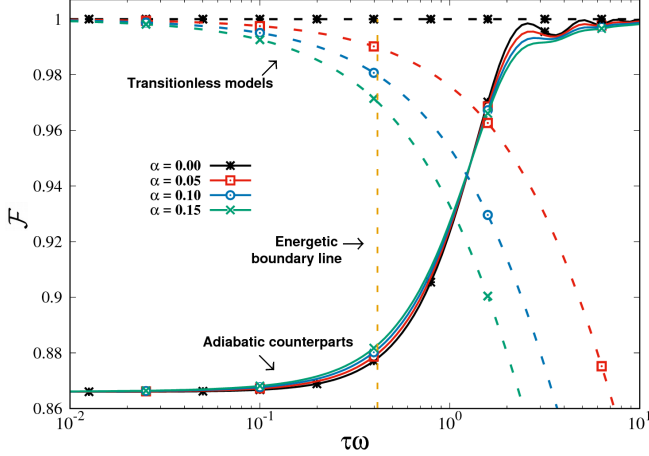


FIG. 6. Fidelity for the adiabatic Landau-Zener model (continuum lines) and its optimal transitionless counterpart (dashed lines) under dephasing, where different energy resources for adiabatic and generalized transitionless evolutions are provided. The vertical dashed line represents the boundary line between  $\Sigma_0(\tau) \leq \Sigma_{SA}(\tau)$  and  $\Sigma_0(\tau) \geq \Sigma_{SA}(\tau)$ .

We further observe that, by fixing the energy cost of the Hamiltonian, fidelity is constrained to be constant in the closed system scenario. This is a direct consequence of Eq. (24). However, in the open system regime, fidelity increases under dephasing, since the adiabatic approximation is not governed by the energy scale of the Hamiltonian but rather by the eigenvalue scale of the Lindbladian [10, 11], which is not fixed. In Fig. 6, it is also exhibited that generalized transitionless evolutions can be more robust in a real open-system scenario even in situations for which the adiabatic implementation has more energy resource available.

#### Appendix D: Transitionless evolution in the quantum gate Hamiltonian

In this section we discuss the details of the transitionless evolution for the quantum gate Hamiltonian  $H_{\text{SQC}}(s) = [\mathbb{1} - P_{11, \hat{n}_-}] \otimes H_0(s) + P_{11, \hat{n}_-} \otimes H_\phi(s)$ , where  $P_{11, \hat{n}_\pm} = |11\rangle\langle 11| \otimes |\hat{n}_\pm\rangle\langle \hat{n}_\pm|$  is a projector over the target system  $\mathcal{T}$ , with  $|\hat{n}_\pm\rangle$  being a state in the direction  $\hat{n}$ , and the Hamiltonian  $H_\xi(s)$  ( $\xi = \{0, \phi\}$ ) acts on the auxiliary system  $\mathcal{A}$ , reading [46]

$$H_\xi(s) = -\omega \{ \sigma_z \cos(\varphi_0 s) + \sin(\varphi_0 s) [\sigma_x \cos \xi + \sigma_y \sin \xi] \},$$

The ground  $|E_{-, \xi}(s)\rangle$  and first excited  $|E_{+, \xi}(s)\rangle$  states of  $H_\xi(s)$  are given by

$$|E_{-, \xi}(s)\rangle = \cos(\varphi_0 s/2)|0\rangle + e^{i\xi} \sin(\varphi_0 s/2)|1\rangle, \quad (25)$$

$$|E_{+, \xi}(s)\rangle = -\sin(\varphi_0 s/2)|0\rangle + e^{i\xi} \cos(\varphi_0 s/2)|1\rangle. \quad (26)$$

The Hamiltonian  $H_{\text{SQC}}(s)$  can be designed to implement quantum gates using controlled evolutions. In particular, the Hamiltonian that adiabatically implements any single-qubit gate for an arbitrary input state  $|\psi\rangle = a|0\rangle + b|1\rangle$ , with  $a, b \in \mathbb{C}$ , is given by [46]

$$H_{\text{sg}}(s) = P_+ \otimes H_0(s) + P_- \otimes H_\phi(s), \quad (27)$$

where  $\{P_\pm\}$  is a complete set of orthogonal projectors over the Hilbert space of the target qubit. The projectors can be parametrized as  $P_\pm = (\mathbb{1} \pm \hat{n} \cdot \vec{\sigma})/2$ , with  $\hat{n}$  associated with the direction of the target qubit on the Bloch sphere. By expressing the state  $|\psi\rangle$  in the basis  $\{|n_\pm\rangle\}$ , we write  $|\psi\rangle = \alpha|n_+\rangle + \beta|n_-\rangle$ , with  $\alpha, \beta \in \mathbb{C}$ . We prepare the system in the initial state  $|\Psi(0)\rangle = |\psi\rangle|0\rangle$ . Then, assuming an adiabatic dynamics, the evolved state  $|\Psi(s)\rangle$  is given by the superposition

$$\begin{aligned} |\Psi(s)\rangle &= \alpha|n_+\rangle|E_{+,0}(s)\rangle + \beta|n_-\rangle|E_{+,\phi}(s)\rangle \\ &= \cos\left(\frac{\varphi_0 s}{2}\right)|\psi\rangle|0\rangle + \sin\left(\frac{\varphi_0 s}{2}\right)|\psi_{\text{rot}}\rangle|1\rangle, \end{aligned} \quad (28)$$

with  $|\psi_{\text{rot}}\rangle = \alpha|n_+\rangle + e^{i\phi}\beta|n_-\rangle$  being the rotated desired state. Therefore, at the end of the evolution, a measurement on the auxiliary qubit yields the rotated state with probability  $\sin^2(\varphi_0/2)$  and the input state with probability  $\cos^2(\varphi_0/2)$ . The computation process is therefore *probabilistic*, which succeeds if the auxiliary qubit ends up in the state  $|1\rangle$ . Otherwise, the target system automatically returns to the input state and we simply restart the protocol. In the adiabatic scenario, the parameter  $\varphi_0$  can then be adjusted in order to obtain the optimal fidelity 1 by taking the limit  $\varphi_0 \rightarrow \pi$ , implying in a deterministic computation. For generalized transitionless evolution, it is possible to show that a probabilistic process with  $\varphi \neq \pi$  is energetically better than the deterministic approach [19].

This model can be easily adapted to implement controlled single-qubit gates. To this end, the target system has to be increased from one qubit to two qubits. Here, we adopt that the single-qubit gate acts on the target register if the state of the control register is  $|1\rangle$ . With this convention, the Hamiltonian that implements a controlled single-qubit gate is given by

$$H_{\text{cg}}(s) = (\mathbb{1} - P_{1,-}) \otimes H_0(s) + P_{1,-} \otimes H_\phi(s), \quad (29)$$

where now the set the orthogonal projectors is given by  $P_{k,\pm} = |k\rangle\langle k| \otimes |n_\pm\rangle\langle n_\pm|$ , where  $|k\rangle$  denotes the computational basis. The input state of the target system is now written as  $|\psi_2\rangle = a|00\rangle + b|01\rangle + c|10\rangle + d|11\rangle$ , with  $a, b, c, d \in \mathbb{C}$  and  $|nm\rangle = |n\rangle|m\rangle$  denoting the control and target register, respectively. By rewriting  $|\psi_2\rangle$  in terms

of the basis  $|n_{\pm}\rangle$ , we have  $|\psi_2\rangle = \alpha|0n_+\rangle + \beta|0n_-\rangle + \gamma|1n_+\rangle + \delta|1n_-\rangle$ . Therefore, by assuming adiabatic evolution, the system evolves from state  $|\Psi_2(0)\rangle = |\psi_2\rangle|0\rangle$ , to the instantaneous state

$$\begin{aligned} |\Psi(s)\rangle &= \alpha|0n_+\rangle|E_{+,0}(s)\rangle + \beta|0n_-\rangle|E_{+,0}(s)\rangle \\ &\quad + \gamma|1n_+\rangle|E_{+,0}(s)\rangle + \delta|1n_-\rangle|E_{+,0}(s)\rangle \\ &= \cos\left(\frac{\varphi_0 s}{2}\right)|\psi_2\rangle|0\rangle + \sin\left(\frac{\varphi_0 s}{2}\right)|\psi_{2\text{rot}}\rangle|1\rangle \end{aligned} \quad (30)$$

with  $|\psi_{2\text{rot}}\rangle = \alpha|0n_+\rangle + \beta|0n_-\rangle + \gamma|1n_+\rangle + e^{i\phi}\delta|1n_-\rangle$  being the rotated desired state. We then see that the final state  $|\Psi(1)\rangle$  allows for a probabilistic interpretation for the evolution and, consequently, the computation protocol can again be taken as probabilistic ( $\varphi_0 \neq \pi$ ) or deterministic ( $\varphi_0 = \pi$ ).

The generalized transitionless Hamiltonians associated with  $H_{\xi}(s)$  can be directly derived from  $H_{\text{SA}}(t)$ . Notice that, from Eq. (25) and (26), it is possible show that Theorem 2 holds, which implies in

$$\begin{aligned} H_{\text{SA},\xi} &= \frac{1}{\tau} \sum_{k=\pm} |d_s E_{k,\xi}(s)\rangle \langle E_k(s)| \\ &= \frac{\varphi_0}{2\tau} [\sigma_y \cos \xi - \sigma_x \sin \xi] \end{aligned} \quad (31)$$

where we have used that  $\langle E_{k,\xi}(s) | d_s E_{k,\xi}(s) \rangle = 0$ , with  $k \in \{+, -\}$ . The Hamiltonian in Eq. (31) improves the transitionless gate Hamiltonian derived in Ref. [17]. More specifically, Eq. (31) is energetically optimal and given by a time-independent operator. Then, we can derive the generalized transitionless Hamiltonians for single-qubit and controlled single-qubit gates as

$$H_{\text{sg}}^{\text{SA}} = P_+ \otimes H_{\text{SA},0} + P_- \otimes H_{\text{SA},\phi}, \quad (32)$$

$$H_{\text{cg}}^{\text{SA}} = (\mathbb{1} - P_{1,-}) \otimes H_{\text{SA},0} + P_{1,-} \otimes H_{\text{SA},\phi}, \quad (33)$$

respectively.

### Energy cost for the quantum gate Hamiltonian

For a fixed amount of energy resource available, our aim is to compare the best adiabatic protocol to implement quantum gates with its best generalized transitionless counterpart. To this end, we will consider the probabilistic model associated with counter-diabatic quantum gates [19]. From Eq. (32), we can write the energy cost to implement single-qubit gates by optimal transitionless evolutions as

$$\Sigma_{\text{SA},\text{sg}}(\tau, \varphi_0) = \frac{\varphi_0}{\omega\tau} \csc^2(\varphi_0/2) \Sigma_{\text{sg}}, \quad (34)$$

where  $\Sigma_{\text{sg}} = 2\omega$  is the adiabatic energy cost and  $\varphi_0$  is the free angle parameter. The choice of  $\varphi_0$  is such that  $\Sigma_{\text{SA},\text{sg}}$  is minimized. In particular, from Eq. (34), minimization is numerically obtained for  $\varphi_0 \approx 0.742\pi$  for any  $\tau$ . It is important mention that the energy cost in

Eq. (34) is obtained by two processes: i) application of the probabilistic model of quantum gates and ii) minimization through the choice of the quantum phase  $\theta_n(t)$  that accompanies the transitionless evolution.

By defining again the energy rate  $\mathcal{R}(\tau, \varphi_0)$  for the adiabatic and generalized transitionless protocol, we have

$$\mathcal{R}(\tau, \varphi_0) = \frac{\Sigma_0(\tau)}{\Sigma_{\text{SA},\text{sg}}(\tau, \varphi_0)} = \frac{\omega\tau}{\varphi_0} \sin^2(\varphi_0/2). \quad (35)$$

By imposing identical energy resource, i.e.  $\mathcal{R}(\tau, \varphi_0) = 1$ , we obtain

$$\omega\tau = \varphi_0 \csc^2(\varphi_0/2). \quad (36)$$

Remarkably, the energy cost for the implementation of a controlled single-qubit gate by the transitionless Hamiltonian in Eq. (33) is simply  $\Sigma_{\text{SA},\text{cg}} = \sqrt{2}\Sigma_{\text{SA},\text{sg}}$ . The factor  $\sqrt{2}$  also propagates to the adiabatic model, which implies exactly in the same ratio  $\mathcal{R}(\tau, \varphi_0)$  and therefore in the same constraint over  $\omega\tau$  provided by Eq. (36).

### Robustness against decoherence in the quantum gate Hamiltonian

From Eq. (35), the optimal transitionless quantum gate model will be more efficient from the energy point of view than its adiabatic counterpart for  $\omega\tau \geq \varphi_0 \csc^2(\varphi_0/2)$ . Even though this condition solves the problem for closed quantum systems, it is a nontrivial problem the energy efficiency of the generalized transitionless quantum gate Hamiltonian in comparison with its adiabatic version when decoherence effects are not negligible in the physical system. In this section we will generalize the results for the robustness of counter-diabatic QC by controlled evolutions against decoherence by considering the case of single-qubit gates in addition to the CNOT gate. We also add dephasing in the instantaneous Hamiltonian eigenbasis, whose Lindblad operator reads  $L_d(s) = U^\dagger(s)\sigma_z U(s)$ , with decoherence rate given by  $\gamma_d \equiv \alpha\omega_r$ . As before,  $\alpha$  denotes a dimensionless parameter and  $\omega_r$  a relevant frequency adopted to parametrize  $\gamma_d$ . The success of the protocol is measured by the fidelity  $\mathcal{F} = \sqrt{\langle \psi_{\text{rot}} | \rho(1) | \psi_{\text{rot}} \rangle}$ , with  $\rho(1)$  denoting the density operator for the target subsystem, obtained from the solution of the master equation. In addition to the CNOT gate presented before we will consider the implementation of the Hadamard phase gate, which read

$$H = \frac{1}{\sqrt{2}} \begin{bmatrix} 1 & 1 \\ 1 & -1 \end{bmatrix}. \quad (37)$$

The CNOT and the Hadamard gate, together with the phase gate and the  $\frac{\pi}{8}$ -gate, can be used to perform universal QC with arbitrary precision [49]. The Hadamard gate is a rotation of  $\pi/2$  around direction  $y$  in the Bloch



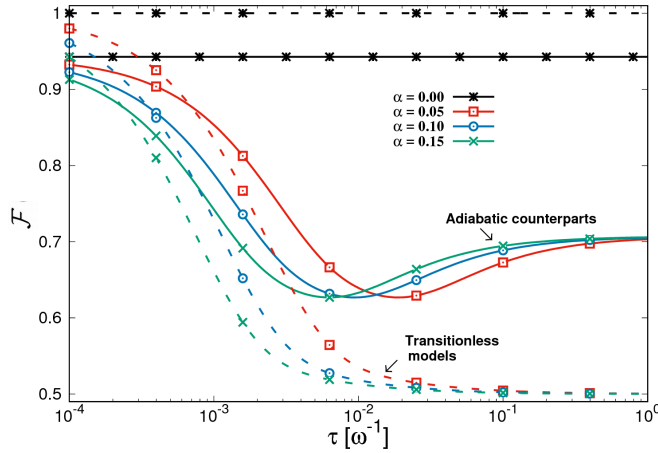


FIG. 7. Fidelity for the adiabatic (continuum lines) and its transitionless dynamics counterpart (dashed lines) implementations for the Hadamard gate under dephasing for identical energy resource.

sphere. Therefore, we obtain the following Hamiltonians for optimal transitionless dynamics

$$H_{SA,0} = \frac{\varphi_0}{2\tau} \sigma_y \quad , \quad H_{SA,\frac{\pi}{2}} = -\frac{\varphi_0}{2\tau} \sigma_x. \quad (38)$$

The robustness of the Hadamard gate under dephasing is illustrated in Fig. 3 for equal resources imposed. In this plot, we compare the optimal adiabatic (deterministic) implementation of the Hadamard gate with its optimal transitionless version (probabilistic computation and optimal quantum phases). Note that, for a fixed  $\alpha$ , the generalized transitionless approach shows a higher fidelity for fast dynamics, with the adiabatic approach exhibiting a better fidelity in the asymptotic limit. In any case, there always exist dynamical regimes for which the optimal transitionless evolutions are more robust and therefore a preferred approach in a decohering physical environment. We observe that this occurs even for a decohering channel that favors the adiabatic model over its generalized transitionless counterpart, such as dephasing and spontaneous emission in the energy eigenstate basis (since the target state is the ground state of the adiabatic Hamiltonian). Similar results are observed for phase gate and the  $\frac{\pi}{8}$ -gate, which allows to extend the conclusion for a universal set of gate Hamiltonians.

\* [ac.santos@id.uff.br](mailto:ac.santos@id.uff.br)

† [msarandy@id.uff.br](mailto:msarandy@id.uff.br)

- [1] M. Born and V. Fock, *Z. Phys.* **51**, 165 (1928).
- [2] T. Kato, *J. Phys. Soc. Jpn.* **5**, 435 (1950).
- [3] A. Messiah, *Quantum mechanics*, North-Holland, Amsterdam (1962).

- [4] J. Jing, M. S. Sarandy, D. A. Lidar, D.-W. Luo and L.-A. Wu, *Phys. Rev. A* **94**, 042131 (2016).
- [5] S. Teufel, *Adiabatic perturbation theory in quantum dynamics*, Lecture Notes in Mathematics **1821**, Springer-Verlag Berlin Heidelberg, 2003.
- [6] S. Jansen, M.-B. Ruskai and R. Seiler, *J. Math. Phys.* **48**, 102111 (2007).
- [7] M. S. Sarandy, L.-A. Wu and D. A. Lidar, *Quantum Information Processing* **3**, 331 (2004).
- [8] J.-d. Wu, M.-s. Zhao, J.-l. Chen, and Y.-d. Zhang, *Phys. Rev. A* **77**, 062114 (2008).
- [9] J. Du, L. Hu, Y. Wang, J. Wu, M. Zhao, and D. Suter, *Phys. Rev. Lett.* **101**, 060403 (2008).
- [10] M. S. Sarandy and D. A. Lidar, *Phys. Rev. A* **71**, 012331 (2005).
- [11] M. S. Sarandy and D. A. Lidar, *Phys. Rev. Lett.* **95**, 250503 (2005).
- [12] M. Demirplak and S. A. Rice, *J. Phys. Chem. A* **107**, 9937 (2003).
- [13] M. Demirplak and S. A. Rice, *J. Phys. Chem. B* **109**, 6838 (2005).
- [14] M. V. Berry, *J. Phys. A: Math. Theor.* **42**, 365303 (2009).
- [15] A. del Campo, *Phys. Rev. Lett.* **111**, 100502 (2013).
- [16] H. Saberi, T. Opatrny, Klaus Molmer and A. del Campo, *Phys. Rev. A* **90**, 060301(R) (2014).
- [17] A. C. Santos and M. S. Sarandy, *Sci. Rep.* **5**, 15775 (2015).
- [18] A. C. Santos, R. D. Silva and M. S. Sarandy, *Phys. Rev. A* **93**, 012311 (2016).
- [19] I. B. Coulamy, A. C. Santos, I. Hen and M. S. Sarandy, *Front. ICT* **3**, 19 (2016).
- [20] M. Beau, J. Jaramillo and A. del Campo, *Entropy* **18**, 168 (2016).
- [21] D. Stefanatos, *Phys. Rev. A* **90**, 023811, (2014).
- [22] M. Lu, Y. Xia, L.-T. Shen, J. Song and N. B. An, *Phys. Rev. A* **89**, 012326 (2014).
- [23] S. Deffner, *New J. Phys.* **18**, 012001 (2016).
- [24] Z.-T. Liang *et al.*, *Phys. Rev. A* **93**, 040305 (2016).
- [25] S. An, D. Lv, A. del Campo and K. Kim, *Nat. Comm.* **7**, 12999 (2016).
- [26] Z. Chen, Y.-H. Chen, Y. Xia and B.-H. Huang, *Sci. Rep.* **6**, 22202 (2016).
- [27] J. Vandermause and C. Ramanathan, *Phys. Rev. A* **93**, 052329 (2016).
- [28] Hao Zhang *et al.*, e-print arXiv:1610.09938 (2016).
- [29] E. Torrontegui *et al.*, *Adv. At. Mol. Opt. Phys.* **62**, 117 (2013).
- [30] J. G. Muga, X. Chen, S. Ibanez, I. Lizuain, and A. Ruschhaupt, *J. Phys. B: At. Mol. Opt. Phys.* **43**, 085509 (2010).
- [31] X. Chen, E. Torrontegui, and J. G. Muga, *Phys. Rev. A* **83**, 062116 (2011).
- [32] M. V. Berry, *Proc. R. Soc. A* **392**, 45 (1984).
- [33] M. Herrera, M. S. Sarandy, E. I. Duzzioni and R. M. Serra, *Phys. Rev. A* **89**, 022323 (2014).
- [34] X. Chen *et al.*, *Phys. Rev. Lett.* **105**, 123003 (2010).
- [35] Y. Zheng, S. Campbell, G. De Chiara and D. Poletti, *Phys. Rev. A* **94**, 042132 (2016).
- [36] S. Campbell and S. Deffner, e-print arXiv:1609.04662 (2016).
- [37] S. Deffner and E. Lutz, *J. Phys. A: Math. Theor.* **46**, 335302 (2013).
- [38] Y.-H. Kang *et al.*, *Sci. Rep.* **6**, 30151 (2016).

- [39] Y.-H. Chen, B.-H. Huang, J. Song and Y. Xia, [Opt. Comm.](#) **380**, 140 (2016).
- [40] B.-J. Liu, Z.-H. Huang, Z.-Y. Xue and X.-D. Zhang, [e-print arXiv:1610.03661](#) (2016).
- [41] J. Jing, L.-A. Wu, M. S. Sarandy, and J. G. Muga, [Phys. Rev. A](#) **88**, 053422 (2013).
- [42] G. Lindblad, [Commun. Math. Phys.](#) **48**, 119 (1976).
- [43] H.-P. Breuer and F. Petruccione, *The theory of open quantum systems*, Oxford University Press, Oxford (2002).
- [44] R. Srikanth and S. Banerjee, [Phys. Rev. A](#) **77**, 012318 (2008).
- [45] C. Cafaro and P. van Loock, [Phys. Rev. A](#) **89**, 022316 (2014).
- [46] I. Hen, [Phys Rev A](#) **91**, 022309 (2015).
- [47] J. M. Martinis and M. R. Geller, [Phys. Rev. A](#) **90**, 022307 (2014).
- [48] R. Barends *et al.*, [Nature](#) **534**, 222 (2016).
- [49] A. Barenco *et al.*, [Phys. Rev. A](#) **52**, 3457 (1995).